E4DVar: Coupling an Ensemble Kalman Filter with Four-Dimensional Variational Data Assimilation in a Limited-Area Weather Prediction Model

MENG ZHANG AND FUQING ZHANG

Department of Meteorology, The Pennsylvania State University, University Park, Pennsylvania

(Manuscript received 26 January 2011, in final form 26 July 2011)

ABSTRACT

A hybrid data assimilation approach that couples the ensemble Kalman filter (EnKF) and four-dimensional variational (4DVar) methods is implemented for the first time in a limited-area weather prediction model. In this coupled system, denoted E4DVar, the EnKF and 4DVar systems run in parallel while feeding into each other. The multivariate, flow-dependent background error covariance estimated from the EnKF ensemble is used in the 4DVar minimization and the ensemble mean in the EnKF analysis is replaced by the 4DVar analysis, while updating the analysis perturbations for the next cycle of ensemble forecasts with the EnKF. Therefore, the E4DVar can obtain flow-dependent information from both the explicit covariance matrix derived from ensemble forecasts, as well as implicitly from the 4DVar trajectory. The performance of an E4DVar system is compared with the uncoupled 4DVar and EnKF for a limited-area model by assimilating various conventional observations over the contiguous United States for June 2003. After verifying the forecasts from each analysis against standard sounding observations, it is found that the E4DVar substantially outperforms both the EnKF and 4DVar during this active summer month, which featured several episodes of severe convective weather. On average, the forecasts produced from E4DVar analyses have considerably smaller errors than both of the stand-alone EnKF and 4DVar systems for forecast lead times up to 60 h.

1. Introduction

Along with the dramatic increase of computing power in recent years, numerical weather prediction (NWP) has become more sophisticated, complementing the deterministic forecast with an ensemble that provides uncertainty estimations of the ''errors of the day.'' Such ensembles also provide a practical way of representing the probability distribution function of forecast uncertainties (also called background errors) that usually propagate in time at multiple scales. In addition, the flow-dependent background error covariance estimated from the ensembles can be used to design better data assimilation approaches, which can also lead to improved forecast skills (Lorenc 2003a). One such approach is the ensemble Kalman filter (EnKF) technique first proposed by Evensen (1994). Meanwhile, three- or four-dimensional variational data assimilation approaches (3D/4DVar) solve the same optimization problem as EnKF and have been widely used in most operational centers for daily forecasts (Parrish and Derber 1992; Courtier et al. 1994). Similar to the EnKF, the estimation of time-evolving error structures has a crucial importance for the success of 4DVar, with the exception of being implicitly described by a linearized model and its adjoint within a short time window (Lorenc 2003b).

In the last decade, the advantages of EnKF and 4DVar data assimilation methods have been demonstrated through various simulated and realistic observation studies, ranging from convective to global scales with different NWP models: (i) for local storms, the EnKF was widely used by Snyder and Zhang (2003), Zhang et al. (2004), Dowell et al. (2004), and Tong and Xue (2005), while Sun and Crook (1997), Guo et al. (2000), and Zupanski et al. (2002) employed 4DVar; (ii) for midlatitude weather systems, the EnKF performed well in Zhang et al. (2006), Torn et al. (2006), Fujita et al. (2007), and Meng and Zhang (2007, 2008a,b), as did 4DVar in Thépaut et al. (1996), Zou and Kuo (1996), Zupanski et al. (2005), and Huang et al. (2002, 2009). Moreover, data assimilation systems employed for real-time or operational global forecasts with either the 4DVar or the EnKF are also promising [e.g., the operational 4DVar at the European

Corresponding author address: Dr. Fuqing Zhang, Department of Meteorology, The Pennsylvania State University, University Park, PA 16802.
E-mail: fzhang@psu.edu

DOI: 10.1175/MWR-D-11-00023.1

© 2012 American Meteorological Society

Centre for Medium-Range Weather Forecasts (ECMWF; Rabier et al. 2000), Japan (Honda et al. 2005), Canada (Gauthier et al. 2007), and the Naval Research Laboratory (NRL; Xu et al. 2005), and several operational or quasi-operational EnKFs in the National Oceanic and Atmospheric Administration (NOAA), Canada, and Japan (Whitaker et al. 2008; Houtekamer et al. 2009; Miyoshi et al. 2010)].

Both of the above data assimilation methods aim to obtain better initial conditions that are more representative of multiscale processes in NWP models. The strengths and weaknesses of EnKF and 4DVar are also very significant (Zhang et al. 2009): EnKF has the advantages of explicit estimation of time-evolving background errors and probabilistic forecasts, but is more vulnerable to sampling errors and also likely to model errors; 4DVar is more flexible for multiscale optimization under linear constraints and has better balance in background error covariance, but such covariance derived from climatological statistics [i.e., the so-called National Meteorological Center (NMC; now known as National Centers for Environmental Prediction) method; Parrish and Derber 1992] is usually static and isotropic and its analysis is only deterministic. Past studies have noted both the benefits of including flow-dependent background error covariance in 4DVar (Rabier et al. 1998; Navon et al. 2005) and the limitations of evolving background uncertainties implicitly through linear models in the presence of strong nonlinearity and discontinuity (Zou 1997; Sun and Crook 1997). Hence, a hybrid approach that combines ensemble-based and variational data assimilation methods may be attractive to most NWP systems (Lorenc 2003a).

A hybrid approach of combining ensemble-based background uncertainties with climatologically derived ones in 3DVar has been previously demonstrated in a quasigeostrophic model by Hamill and Snyder (2000) without covariance localization. Lorenc (2003a) proposed the use of an alpha-control variable transform that enables preconditioning of variational minimization based on ensemble perturbations with localized flow-dependent information. This method was adopted by Buehner (2005) and Wang et al. (2007) for constructing 3DVar–EnKF hybrid systems based on global models. More recently, Wang et al. (2008a,b) successfully used the alpha-control variable transform in a regional-scale NWP model [i.e., the Weather Research and Forecasting model (WRF; Skamarock et al. 2005)] with a simple recursive filter (Hayden and Purser 1995) for modeling ensemble correlations rather than truncated spectral expansion as in Buehner (2005). With the incorporation of flow-dependent background error covariance from an ensemble transform Kalman filter (ETKF; Bishop et al. 2001), the hybrid method (ETKF–3DVar) of Wang et al. performed better than 3DVar in real-data cases though with a relatively coarse grid resolution. More recently, Liu et al. (2008, 2009) implemented an ensemble-based data assimilation (DA) method that uses 4DVar optimization to produce a balanced analysis without tangent-linear and adjoint models, which is essentially another form of linear approximation for time-evolving error structures with ensemble forecasts. Buehner et al. (2010a,b) investigated various ensemble-based and variational methods in a quasi-operational scenario for the Canadian global model, but the ensemble members were fully updated by EnKF (one-way coupled) without replacing the mean with a variational analysis, as proposed in Lorenc (2003a). It is important to note that the aforementioned hybrid approaches depend largely on the quality of ensembles, so typical issues associated with the EnKF, such as sampling and model errors and/or filter divergence, still exist.

Two-way coupling of the 4DVar with EnKF (i.e., E4DVar) can be viewed as an extension to previously published hybrid methods, but with the advantages of using ensemble-based flow-dependent covariance and model-constrained trajectory analysis. Preliminary results of this method were shown in Zhang et al. (2009) for a simple Lorenz-96 model in both perfect- and imperfect-model scenarios, where the E4DVar approach was shown to be more effective than traditional 4DVar and EnKF methods at reducing root-mean-square error (RMSE), even with an ensemble size as small as 10. In this study, the E4DVar is adapted to a nonhydrostatic regional-scale NWP model (WRF), whose EnKF and 4DVar modules were proven to be fully functional and robust in previous studies (Meng and Zhang 2008a,b; Huang et al. 2009; Zhang et al. 2011). Several one-month analysis/forecast experiments with different DA methods are conducted, where most if not all available conventional observations other than satellite radiances are assimilated over a domain that spans much of North America. The hybrid formulations are shown in section 2, followed by experiment design in section 3. The experiments results are discussed in section 4 and conclusions are summarized in section 5.

2. Hybrid algorithm

a. Incremental 4DVar

Mathematically, the variational method is aimed at obtaining a balanced state analysis subject to both dynamical and statistical constraints by minimizing a cost function J:

$$J = \frac{1}{2}\delta\mathbf{x}_0^{\mathrm{T}}\mathbf{B}^{-1}\delta\mathbf{x}_0 + \frac{1}{2}\sum_{k=0}^{K}(\mathbf{H}_k\mathbf{M}_k\delta\mathbf{x}_0 - \mathbf{d}_k)^{\mathrm{T}} \times \mathbf{R}^{-1}(\mathbf{H}_k\mathbf{M}_k\delta\mathbf{x}_0 - \mathbf{d}_k) + J_c, \quad (1)$$

where the three right-hand-side terms are the background J_b, observational J_o, and penalty J_c cost functions, respectively, and the subscript k denotes an observational time during the assimilation window. In the background term J_b, $\delta\mathbf{x}_0$ is the analysis increments at the initial time from first guess and $\mathbf{B}$ is the background error covariance. In the observational term J_o, $\mathbf{M}_k$ and $\mathbf{H}_k$ are the tangent linear versions of the forecast model and observation operator, $\mathbf{R}$ is the observational error covariance, and $\delta\mathbf{x}_k$ and $\mathbf{d}_k = \mathbf{y}_k^o - \mathbf{H}_k\mathbf{x}_k$ are the perturbation and innovation vectors distributed at time k during the assimilation window of length K. In J_c, a digital filter (Gauthier and Thépaut 2001) is introduced to remove high-frequency waves in the analysis state. For the incremental approach (Courtier et al. 1994; Gauthier et al. 2007), an outer loop is used to calculate the innovations $\mathbf{d}_k$, and the iterative minimization is performed only on linearized models. The preconditioning of the background term in the cost function (Courtier et al. 1994; Courtier 1997; Andersson et al. 2000) is conducted with a control variable $\boldsymbol{v}$ (Lorenc et al. 2000; Barker et al. 2004):

$$\delta\mathbf{x}_0 = \mathbf{U}\boldsymbol{v}, \tag{2}$$

where the preconditioning matrix $\mathbf{U}$ is defined as $\mathbf{B} = \mathbf{U}\mathbf{U}^{\mathrm{T}}$. Then the incremental formulation of the cost function (1) is adapted as

$$J = \frac{1}{2}\boldsymbol{v}^{\mathrm{T}}\boldsymbol{v} + \frac{1}{2}\sum_{k=0}^{K}(\mathbf{H}_k\mathbf{M}_k\mathbf{U}_k\boldsymbol{v} - \mathbf{d}_k)^{\mathrm{T}}\mathbf{R}^{-1}(\mathbf{H}_k\mathbf{M}_k\mathbf{U}_k\boldsymbol{v} - \mathbf{d}_k) + J_c. \tag{3}$$

b. EnKF

For the standard ensemble Kalman filter, the update equations can be formulated as

$$\overline{\mathbf{x}}^a = \overline{\mathbf{x}}^f + \mathbf{K}(\mathbf{y} - \mathbf{H}\overline{\mathbf{x}}^f), \tag{4}$$

$$\mathbf{X}^a = \mathbf{X}^f + \mathbf{K}(\mathbf{y} - \mathbf{H}\mathbf{X}^f), \tag{5}$$

$$\mathbf{P}^f \approx \overline{\mathbf{x}'^f(\mathbf{x}'^f)^{\mathrm{T}}} = \frac{1}{N-1}\sum_{i=1}^{N}(\mathbf{x}_i^f - \overline{\mathbf{x}^f})(\mathbf{x}_i^f - \overline{\mathbf{x}^f})^{\mathrm{T}}, \tag{6}$$

$$\mathbf{K} = \mathbf{P}^f\mathbf{H}^{\mathrm{T}}(\mathbf{H}\mathbf{P}^f\mathbf{H}^{\mathrm{T}} + \mathbf{R})^{-1}, \tag{7}$$

where $\overline{\mathbf{x}}^f$ ($\mathbf{X}^f$) and $\overline{\mathbf{x}}^a$ ($\mathbf{X}^a$) represent the prior and posterior mean vector (perturbation matrix) (or first guess and analysis) at the analysis time, respectively; i denotes the order of an ensemble member; and N is the ensemble size. Here $\mathbf{K}$ is the so-called Kalman gain matrix, where $\mathbf{P}^f$ represents the background error covariance, which is referred to as $\mathbf{B}$ in 4DVar. A flow-dependent $\mathbf{P}^f$ is estimated through an ensemble of short-range forecasts by (6). Observations are assimilated sequentially with the assumption of independent observational errors (i.e., refers to the square root EnKF in Snyder and Zhang 2003).

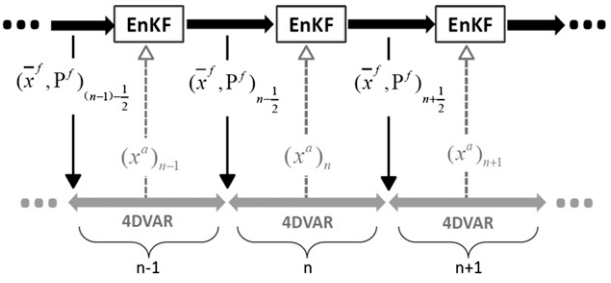

FIG. 1. Schematic of E4DVar that couples 4DVar and EnKF.

c. E4DVar

In the E4DVar, 4DVar and EnKF run separately in parallel but also with two-way exchanges. There is a "coupler" between them that contains three major variable exchanges (Fig. 1): (i) introduce ensemble-based background error covariance $\mathbf{P}^f$ into the 4DVar cost function, (ii) use prior ensemble mean $\overline{\mathbf{x}^f}$ as the first guess for each 4DVar cycle,[1] and (iii) replace posterior ensemble mean by the 4DVar analysis $\mathbf{x}_0^a$ for next ensemble forecast (Zhang et al. 2009).

The ensemble-based background error covariance is introduced in the cost function by separating J_b in (1) into two parts:

$$J_b = J_{\mathrm{b1}} + J_{\mathrm{b2}} = \frac{1}{2}\delta\mathbf{x}_0^{\mathrm{T}}[(1-\beta)\mathbf{B} + \beta\mathbf{P}_0^f \circ \mathbf{C}]^{-1}\delta\mathbf{x}_0, \tag{8}$$

where $\mathbf{P}_0^f$ is the prior ensemble covariance valid at the analysis time (i.e., the beginning of the assimilation window), $\mathbf{C}$ is a block-diagonal matrix representing the ensemble covariance localization (Lorenc 2003a; Wang et al. 2007, 2009), "$\circ$" represents a Schur product, and J_{b1} represents the traditional background term as in (1), which can be weighted with the ensemble-based term J_{b2}

[1] The alternative is to use the previous 4DVar forecast as the first guess as suggested by one of the reviewers to avoid potential issues of flow imbalance by using an ensemble mean. However, our limited sensitivity experiments with this alternative give slightly inferior performances. On the other hand, there were no apparent flow imbalance problems by using the ensemble mean in the current study, which may not always be true in higher resolutions.

using the weighting coefficient β. The hybrid formulation approaches the standard 4DVar when $\beta \to 0$, while the ensemble 4DVar (i.e., En4DVar; see Liu et al. 2008, 2009; Buehner et al. 2010a,b) emerges for $\beta \to 1$. When the alpha-control variable transform is applied, the hybrid incremental analysis can be calculated as the traditional control variable $\boldsymbol{v}$ (associated with the NMC-based covariance; Barker et al. 2004) supplemented by the additional control variable $\boldsymbol{\alpha}$ (associated with the ensemble-based covariance; Lorenc 2003a):

$$\delta\mathbf{x}_0 = \delta\mathbf{x}_{\text{nmc}} + \delta\mathbf{x}_{\text{ens}} = \mathbf{U}\boldsymbol{v} + \mathbf{X}^f\boldsymbol{\alpha}. \tag{9}$$

The cost function (1) can be rewritten as

$$J = \frac{1}{1-\beta}\left(\frac{1}{2}\boldsymbol{v}^{\mathrm{T}}\boldsymbol{v}\right) + \frac{1}{\beta}\left[\frac{1}{2}\boldsymbol{\alpha}^{\mathrm{T}}\begin{pmatrix}\mathbf{C} & & \mathbf{0}\\ & \cdots & \\ \mathbf{0} & & \mathbf{C}\end{pmatrix}\boldsymbol{\alpha}\right] + \frac{1}{2}\sum_{k=0}^{K}(\mathbf{H}_k\mathbf{M}_k\delta\mathbf{x}_0 - \mathbf{d}_k)^{\mathrm{T}}\mathbf{R}^{-1}(\mathbf{H}_k\mathbf{M}_k\delta\mathbf{x}_0 - \mathbf{d}_k) + J_c. \tag{10}$$

3. Experiment design

a. Forecast model

In this study, the Advanced Research WRF model (ARW-WRF; Skamarock et al. 2005) is employed as the platform to investigate all DA approaches. The WRF configuration is exactly the same as in Zhang et al. (2011). All experiments are conducted over a single domain covering the contiguous United States and surrounding areas (Fig. 2) that has a 71 × 51 horizontal mesh grid with 90-km spacing and 27 vertical levels up to 50 hPa. The Grell–Devenyi cumulus scheme (Grell and Devenyi 2002), the WRF single-moment six-class graupel microphysics scheme (Hong et al. 2004), and the Yonsei State University (YSU) planetary boundary layer (PBL) scheme (Noh et al. 2003) are used for all deterministic forecasts. In the ensemble forecast, we used different combinations of different physics parameterization schemes in different ensemble members (multiphysics ensemble) configured exactly the same as in Meng and Zhang (2008a,b). The first forecast cycle of this month-long experiment is initialized at 0000 UTC 1 June 2003, using the National Centers for Environmental Prediction (NCEP) global final analysis (FNL) data to create the initial and lateral boundary conditions (ICs and LBCs). In the following cycles, LBCs are interpolated from the FNL analyses, while ICs are provided by analyses produced by the tested DA schemes.

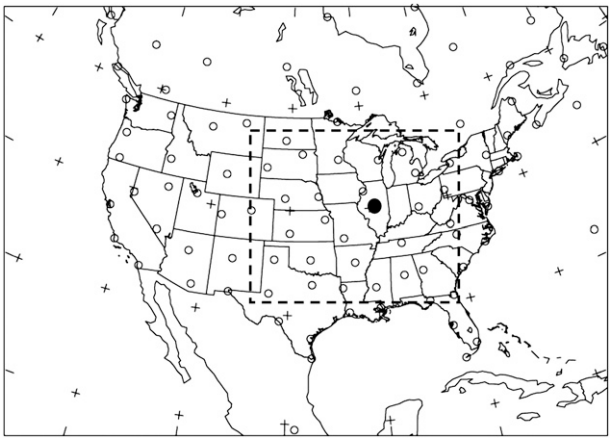

FIG. 2. Model domain configuration. The open circles denote the locations of the radiosonde observations used for assimilation and verification. The dashed box shows the sublet of the domain selected for verification statistics. The solid circle marks the location of the single-observation experiment.

b. Data assimilation systems

The data assimilation systems described here in this section are based on the WRF variational data assimilation system (WRF-Var) version 3 (Barker et al. 2004; Huang et al. 2009) and the WRF EnKF of Meng and Zhang (2008a,b). The newly released 4DVar component (Huang et al. 2009) of WRF-Var was developed as an extension of the previous WRF 3DVar system (Barker et al. 2004). The background error covariance in the 4DVar experiment is static and prescribed by the NMC method (Parrish and Derber 1992), which assumes homogeneous and isotropic correlations for a set of independent control variables (using the "cv5" option in WRF-Var), including streamfunction, velocity potential, unbalanced pressure, and relative humidity. The NMC-based background error covariance is derived from the differences between 24- and 12-h forecasts valid at the same time (i.e., every 0000 and 1200 UTC) during the preceding month (May 2003) before the experiment period. As for the variance and length scale parameters of the derived background error covariance, only the nondimensional variance values of 1.0 (default value) and 3.0 are examined in the 4DVar experiments. The larger value means less confidence is given to the background state (i.e., first guess), which leads to the 4DVar analysis fitting the observations more closely.

The stand-alone EnKF experiment is the same as in Zhang et al. (2011), which adopts similar settings from Meng and Zhang (2008a,b), that is, an ensemble size of 40, with different physical parameterization schemes that differ between members, a relaxation coefficient of 0.8 [Eq. (5) of Zhang et al. (2004)], and prespecified

covariance localizations (Gaspari and Cohn 1999) with a radius of influence of 1800 km for radiosondes and profilers and 600 km for all other observations. Vertical covariance localization of 15 vertical grid points is applied to discrete, single-level observations such as surface data and satellite winds. The initial ensemble perturbations are randomly generated at 0000 UTC 1 June 2003 through the cv5 background error covariance option of the WRF-Var system, which are dynamically balanced by the same set of control variables as in the NMC method (Barker et al. 2004). The perturbations are then added to the FNL analysis to form an initial ensemble, which is then integrated for 12 h to evolve a flow-dependent background error covariance matrix before the first assimilation cycle at 1200 UTC 1 June 2003. The LBCs for the ensemble forecasts are perturbed from the FNL analyses at every analysis time, in the same manner as the initial perturbations.

For the coupling of the 4DVar with EnKF, an alpha-control variable transform (Lorenc 2003a) adapted to WRF-Var (Wang et al. 2008a,b) is applied for all E4DVar experiments. In addition, the information exchanged between the 4DVar and EnKF in the hybrid E4DVar system is controlled by a coupler that is completely separate from the original WRF-Var and EnKF codes, as illustrated by the algorithm in Fig. 1. To reduce the impacts of sampling errors, the same radius of influence (i.e., 1800 km) for horizontal covariance localization is applied in the E4DVar through a simple recursive filter (Hayden and Purser 1995) available in WRF-Var. Moreover, the coefficient for weighting the NMC- and ensemble-based background error covariance estimates is set to 0.8 and 0.5 in this study as suggested in Wang et al. (2008b). Sensitivity experiments performed by the authors suggest that the E4DVar is not very sensitive to this empirical factor (not shown), unlike the 3DVar and ETKF hybrid as in Wang et al. (2009).

c. Observations

Various types of meteorological observations are assimilated by each system, including wind, temperature, and moisture from radiosondes, ships, and surface stations, wind from profilers, wind and temperature from aircrafts, and cloud-tracked wind from satellites. The observation preprocessing modular (OBSPROC) of WRF-Var (Barker et al. 2004) is implemented for data sorting, quality control and observational error assignment for all DA experiments. The first analysis time is at 1200 UTC 1 June 2003, and each DA system continuously cycles through a 6-h analysis/forecast cycle (every 0000, 0600, 1200, and 1800 UTC) until the end of the month. Note, the assimilation window of 4DVar covers the period from −3 to +3 h of each analysis time; therefore, all available observations distributed over a 6-h window can be assimilated, so as in the EnKF except for those locations that have more than one observation over the 6-h window in which case only the one closest to the synoptic time is assimilated. In E4DVar (Fig. 1), the ensemble-based background error covariance $\mathbf{P}^f$ and prior ensemble mean $\overline{\mathbf{x}}^f$ are introduced at the beginning of the 4DVar assimilation window (i.e., 3 h before the analysis time), which are computed from the short-term ensemble forecasts of the previous cycle (i.e., 3-h ensemble forecasts). In return, the 4DVar analysis at −3 h is integrated from the beginning of the assimilation window to the analysis time (i.e., 3-h deterministic forecast) to replace the posterior ensemble mean for the next set of ensemble forecasts. Therefore, the same observations are assimilated for each DA system during their analysis/forecast cycles.

4. Flow-dependent error covariances determined from single-observation experiments

Single-observation experiments were conducted to demonstrate the capability of each DA method on resolving the structure of flow-dependent background error covariance. Similar to the method described in Huang et al. (2009), the impact of assimilating a temperature observation at 500 hPa over Illinois (the location of which is marked in Fig. 2) with a +1-K innovation is examined at the end of a 6-h window for all experiments at 0000 UTC 8 June 2003 in 4DVar, but alternatively at the analysis time for the 3DVar and EnKF. The resulting analysis increments of temperature, horizontal winds, and moisture from various DA experiments are illustrated in Fig. 3, including the outcomes from the 4DVar, EnKF, and E4DVar experiments with 40 and 10 members (referred to as EnKF-40m, EnKF-10m, E4DVar-40m, and E4DVar-10m, respectively). We also show the analysis increments for 3DVar here to illustrate the structure of static isotropic background error covariance for comparison. The 40-member ensemble perturbations valid at 0000 UTC 8 June 2003 were directly extracted from the month-long EnKF experiment with a covariance localization radius of 1800 km (more in the next section). The same 10 ensemble perturbations for both EnKF-10m and E4DVar-10m are randomly chosen from the 40 members, which will have large sampling errors.

In the 3DVar (Fig. 3a), the computed analysis increments have an isotropic structure, centered at the observation location and completely independent of the background flow, because the NMC-based background error covariance in 3DVar is obtained using averaged error statistics (over the previous month in this case), which assumes homogenous and isotropic correlations.

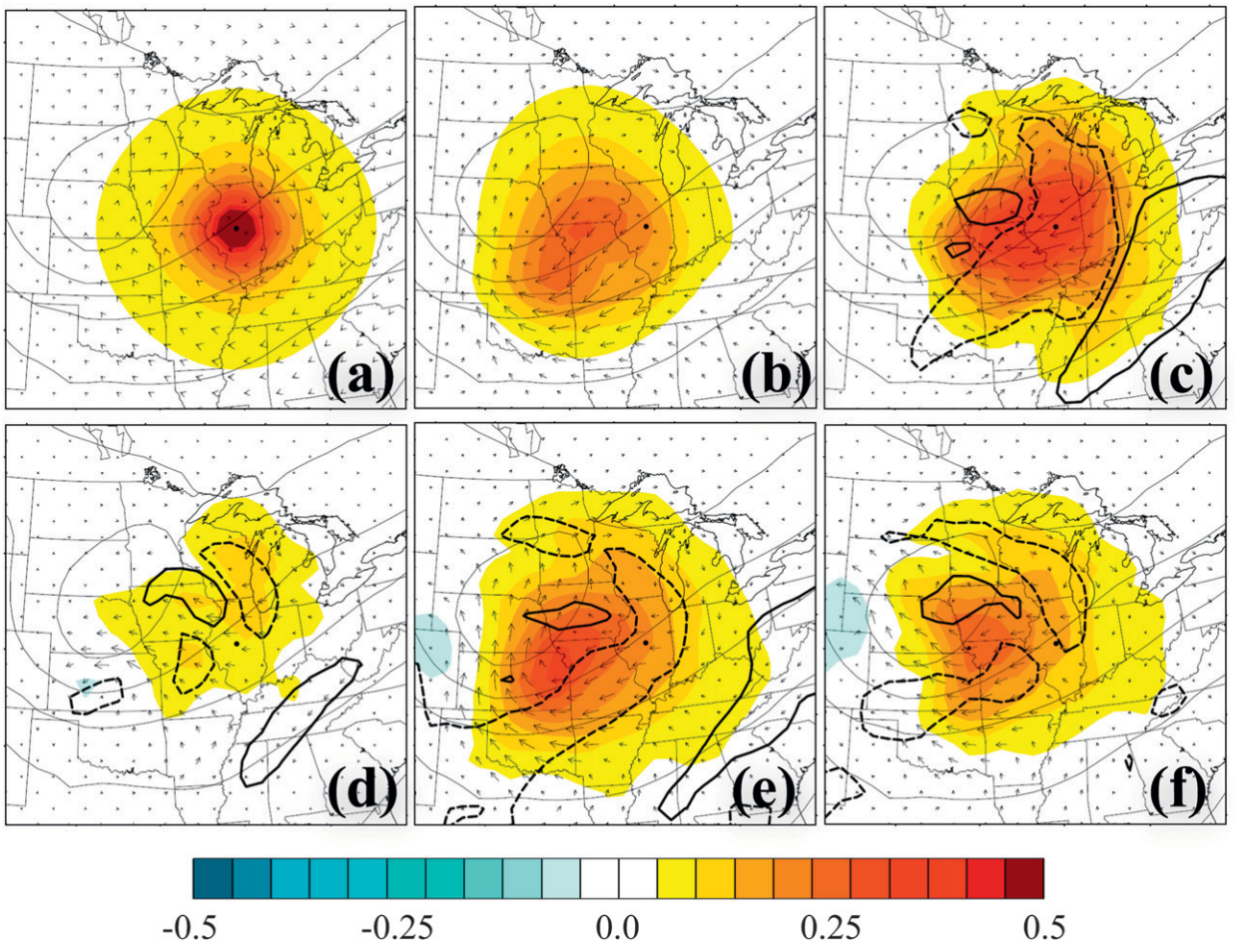

FIG. 3. The DA analysis increments of temperature (shaded, units in K), winds (vectors), and moisture (thick contours, units in g kg^{-1}, solid for positive and dashed for negative) for 1-K innovation at 500 hPa over Illinois (black dot) for (a) 3DVar, (b) 4DVar, (c) EnKF with 40 members, (d) EnKF with 10 members, (e) E4DVar with 40 members, and (f) E4DVar with 10 members. Thin contours are background geopotential height (unit in m).

In contrast, flow-dependent forecast uncertainty and correlations are taken into account during the 4DVar assimilation (Fig. 3b), with the largest temperature increments shifted upstream and the wind increments located southwest along the background geopotential height contours. There are virtually no moisture increments in the 3DVar analysis as no multivariate correlations exist between moisture and other variables in the NMC-based background error covariance of the current WRF-Var, though such correlations could play an important role in severe weather systems. A similar situation is shown in the 4DVar experiment, but with some weak increments to moisture variables that were gained through the linear model iterations. However, with only very simple physics included in the linearization process of 4DVar (Huang et al. 2009), the moisture increments were an order of magnitude smaller than those from EnKF and thus were not plotted in Fig. 3b. Compared to the 4DVar, even stronger flow-dependent analysis increments result from the EnKF with 40 ensemble members (Fig. 3c), including stronger temperature increments and northeasterly wind increments. For a perfect linear system with Gaussian error statistics, the 4DVar and Kalman filter may generate equivalent solutions of the time-evolving error covariance, which can be implicitly modeled through a finite-time window or explicitly estimated by a group of ensemble members (Lorenc 2003b). One major advantage of using ensemble-based background error covariance in the EnKF is the estimation of multivariate correlations between humidity and other state variables as shown in Figs. 3c–f. Note that the representation of cross covariances between temperature and moisture could be highly impacted by the physical parameterizations (Berre 2000), as accounted for by the model errors. However, if only a small ensemble size is used, sampling errors may contaminate the background uncertainty

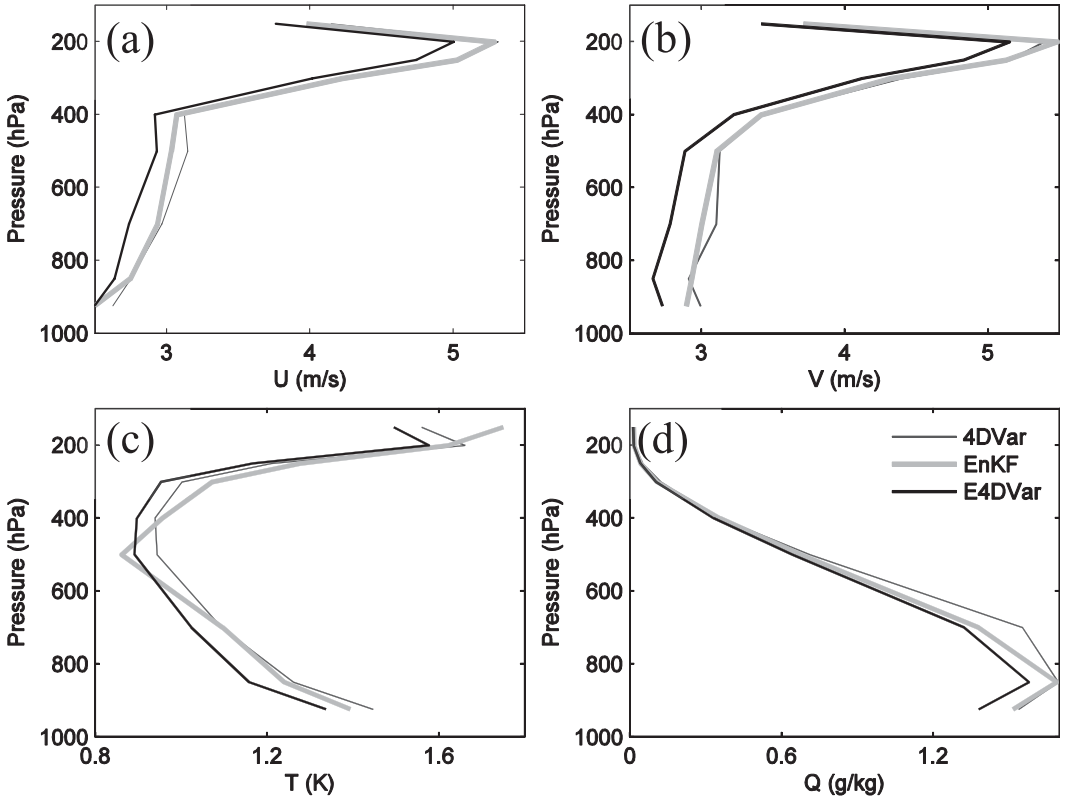

FIG. 4. Vertical profiles of the month-averaged 12-h forecast RMSEs of (a) U (m s^{-1}), (b) V (m s^{-1}), (c) T (K), and (d) Q (g kg^{-1}) for various DA methods.

estimate, even after applying a tighter localization (e.g., Fig. 3d). This would result in a less reliable estimate of forecast covariance, followed by inappropriate analysis increments.

The E4DVar benefits from the relative strengths of both the 4DVar and EnKF, by combining ensemble-based and model-constrained flow-dependent information for the analysis. In the E4DVar with 40 ensemble members (Fig. 3e), the upstream temperature increments are further enhanced by the ensemble-based background error covariance. The ensemble-based covariance introduced a similar northerly wind increment as the stand-alone EnKF, while adding more detail to the entire wind field. In the meantime, the moisture increments are also introduced as in the EnKF. At the same time, through the model-constrained evolution of the covariance matrix [see Eq. (6) in Buehner et al. (2010a)], the analysis increments of the E4DVar using only 10 ensemble members (Fig. 3f) show similar flow-dependent structures as in the 40-member E4DVar. Note that the weighting factor β can be used to control the relative weights of NMC- and ensemble-based background error covariance in the E4DVar system [(8)]. These single-observation experiments are designed to show how flow-dependent background error covariance evolves in different DA systems. It is beyond our capacity to verify whether all the flow-dependent, anisotropic details in the resulting analysis increments are profitable to the analysis. In the following section, the benefits of the coupled system for assimilating real-data observations will become more evident.

5. Intercomparison of E4DVar with EnKF and 4DVar in a one-month experiment

In this section, the E4DVar system is compared with the EnKF and 4DVar systems over the full one-month period to examine its performance relative to the stand-alone methods. We will verify the analyses and deterministic forecasts from the different DA systems with standard sounding observations in which the RMSEs of horizontal winds (U, V), temperature T, and the mixing ratio of water vapor Q are calculated within the selected region shown in Fig. 2; the same verifying domain is used in Meng and Zhang (2008b) and Zhang et al. (2011).

Based on the comparisons of 12-h forecast error profiles (Fig. 4), the E4DVar produces the overall lowest RMSEs for both the wind and thermodynamic variables throughout the troposphere. The EnKF and

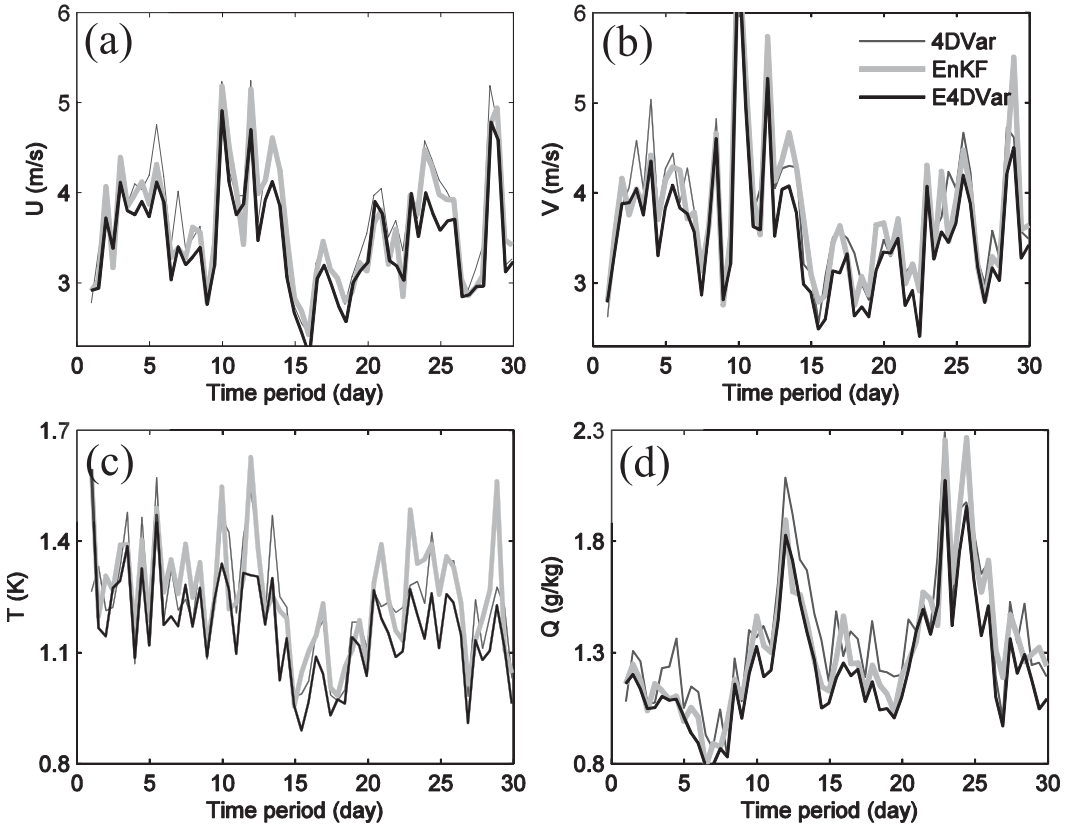

FIG. 5. Time evolution of the vertical-averaged 12-h forecast RMSE of (a) U (m s^{-1}), (b) V (m s^{-1}), (c) T (K), and (d) Q (g kg^{-1}).

the 4DVar performed similarly, except that the EnKF has substantially smaller errors in the moisture analysis (as well as slightly lower errors in winds and temperature). The vertical variations of RMSEs demonstrate that the maximum errors for U, V, and T are at or near the tropopause level (around 200 hPa), while at lower troposphere for moisture. The temporal variations of 12-h forecast RMSEs for different variables are presented in Fig. 5. In agreement with Fig. 4, the E4DVar, in general, has consistently lower forecast errors at most forecast times during the entire month. The relative amplitudes in RMSE for the EnKF- and the 4DVar-initialized forecasts fluctuate considerably and episodically, though the EnKF has smaller RMSEs most of the time, especially in the moisture field.

Model error and biases, especially those arriving from deficiencies in physical parameterization schemes, may significantly degrade the performance of any DA method (Whitaker et al. 2008). Figure 6 shows the vertical distribution of the averaged 12-h forecast biases initialized from different DA analyses. To our surprise, the 12-h forecast biases in all forecast variables are 5–10 times smaller than the 12-h RMSEs. The difference in forecast biases between different DA schemes appears to be inconsequential to the difference in the performance during this month.

Another key aspect of an ensemble-based DA system is the consistency between the forecast (prior) ensemble spread and error. For simplicity, we compare the ensemble spread versus analysis/forecast error in terms of root-mean-difference total energy (RM-DTE) in which the DTE is calculated as in Zhang et al. (2002, 2006): $\mathrm{DTE} = 0.5(U'U' + V'V' + kT'T')$, where the prime denotes the difference between the observations and verified fields, and $k = C_p/T_r$ ($C_p = 1004.7$ J kg^{-1} K^{-1} and the reference temperature T_r is 290 K).

The averaged vertical profiles of ensemble spread versus error in terms of RM-DTE for both the E4DVar and the EnKF are shown in Fig. 7. Overall, the 12-h forecast ensemble spreads for both the EnKF and E4DVar are noticeably smaller than the RM-DTE, although it can still be considered adequate if the observation errors are accounted for, which implies the RM-DTE would be similar to the sum of background and observation error variances [refer to discussion in Meng and Zhang (2008b)]. Nevertheless, the E4DVar does

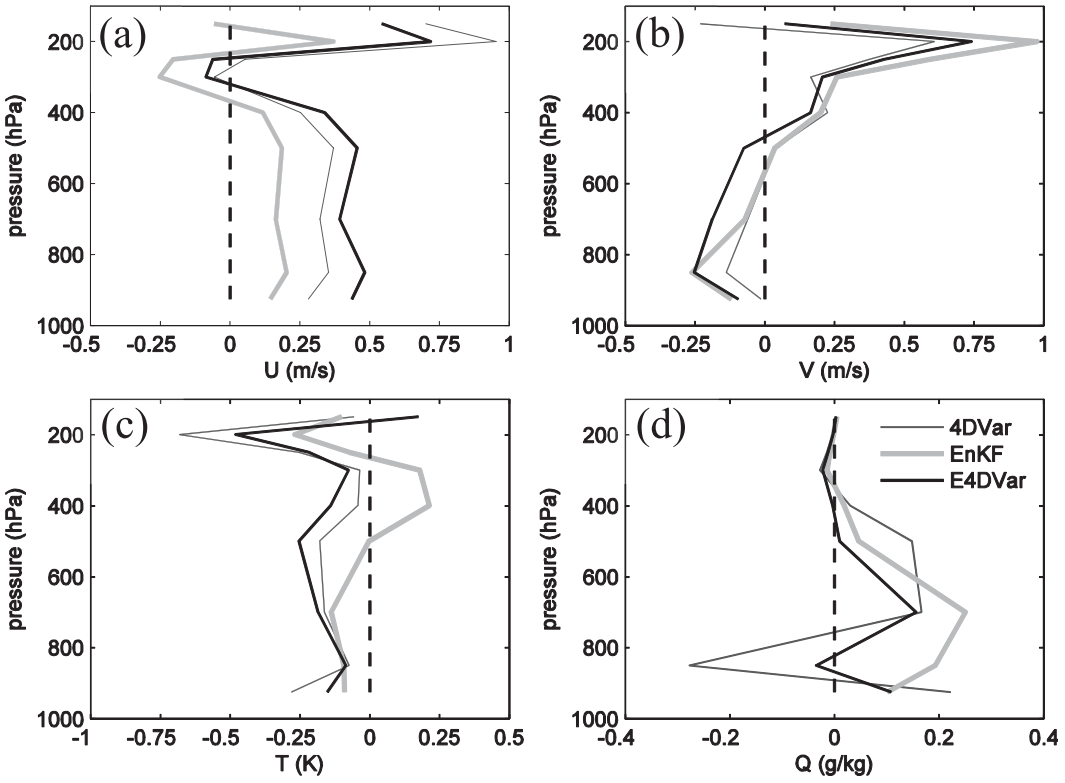

FIG. 6. Vertical profiles of the month-averaged 12-h forecast biases of (a) U (m s^{-1}), (b) V (m s^{-1}), (c) T (K), and (d) Q (g kg^{-1}) for various DA methods.

have slightly but systematically larger ensemble spread than the stand-alone EnKF through the vertical domain (Fig. 7a) and throughout the month (not shown), which is in contrast to a smaller forecast error for the E4DVar (Fig. 7b). The larger ensemble spread in the E4DVar may be a result of an improved estimate of the mean that has enhanced flow uncertainties and a better treatment of the model error (through including NMC-based background covariance) that provides more comprehensive error growth modes in the ensemble, and/or due to a small degree of filter divergence in the stand-alone EnKF system with underestimated background error uncertainties. Note that the inflation parameters have been tuned to optimize the EnKF performance based on several sensitivity tests (not shown), but the inflated uncertainty estimate did not lead to lower forecast errors in this case. On the other hand, the larger ensemble spread in the E4DVar may in turn lead to a better

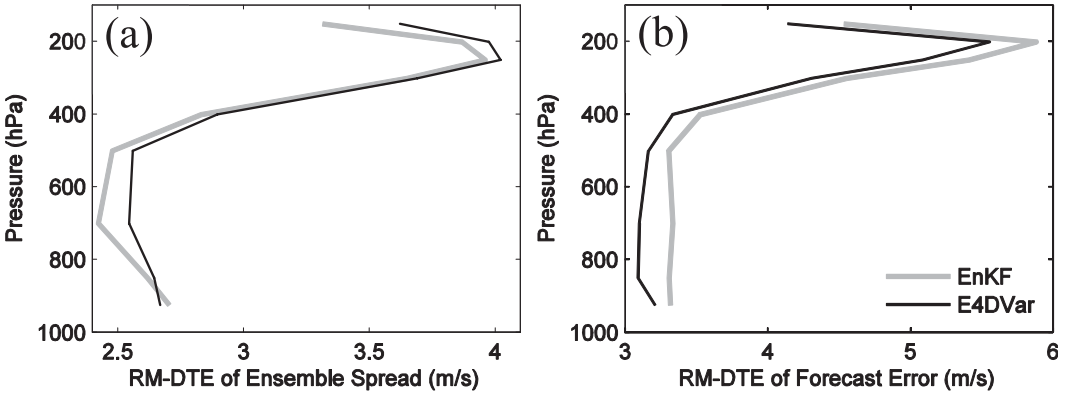

FIG. 7. The month-averaged vertical profiles of the RM-DTE (m s^{-1}) for (a) 12-h ensemble spread and (b) 12-h forecast error.

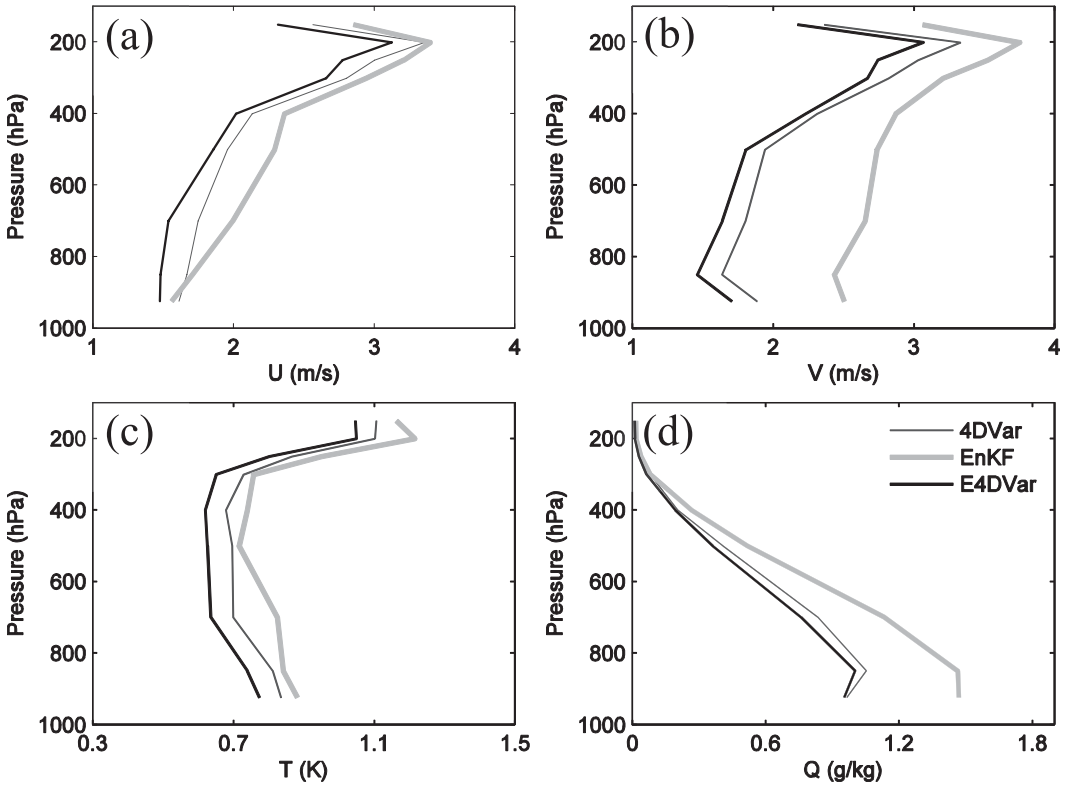

FIG. 8. As in Fig. 4, but for the analysis RMSs fit to observations.

analysis. In essence, increasing the background uncertainty (ensemble spread) in the E4DVAR (as well as in 4DVar and EnKF) can allow a better fit to observations in the assimilation window thereby introducing more dynamical information in the analysis. This at least partially explains the better performance of the E4DVAR over 4DVar (besides the use of flow-dependent error covariance), although a better fit to observation does not always mean a better analysis or lead to a better forecast (refer to Zhang et al. 2011).

Figure 8 shows the vertical profiles of the RMS differences between the DA analyses and the sounding observations. Since all these soundings are assimilated in the analysis, these RMS differences represent the extent to which each DA approach fits the assimilated observations (often termed as ''analysis fit'' or simply ''fit'') rather than providing an independent verification of the analysis quality. In some applications such as for air quality modeling, a better fit of meteorological variables to observations is often desirable. However, the EnKF analysis is often found to have a worse fit than variational methods (e.g., Zhang et al. 2011), likely due to the latter's use of a cost function that minimizes iteratively the distance between the analysis and observations (the observational cost function J_o) with less confidence on the first guess (i.e., larger variance in the NMC-based background error covariance). With the coupling between the EnKF and 4DVar, the E4DVar has the closest fit to observations among all three schemes throughout the vertical domain, by increasing the total variance and allowing better fit with more flow-dependent information on the background term. However, as demonstrated in Zhang et al. (2011), a better analysis fit does not necessarily lead to a better forecast without proper estimation of flow-dependent background error covariance. In this case, the 4DVar with static NMC-based covariance has a considerably closer fit to observations than the EnKF, but with larger forecast errors (Fig. 4).

The same forecast error statistics are computed at different lead times for all DA experiments, from 0 (i.e., analysis) to 72 h (Fig. 9). Based on the results in Zhang et al. (2011), the 4DVar and EnKF mostly outperform 3DVar, with the exception of moisture field corrections, where the multivariate correlations are not included in WRF-Var system for the 3DVar and 4DVar. The 4DVar benefits obtained from a model-constrained trajectory fitting also weaken after 60 h for the U, V, and T variables. The analysis RMSEs of the EnKF are relatively high, but after 24 h the EnKF's advantage of explicitly introducing flow-dependent multivariate uncertainties

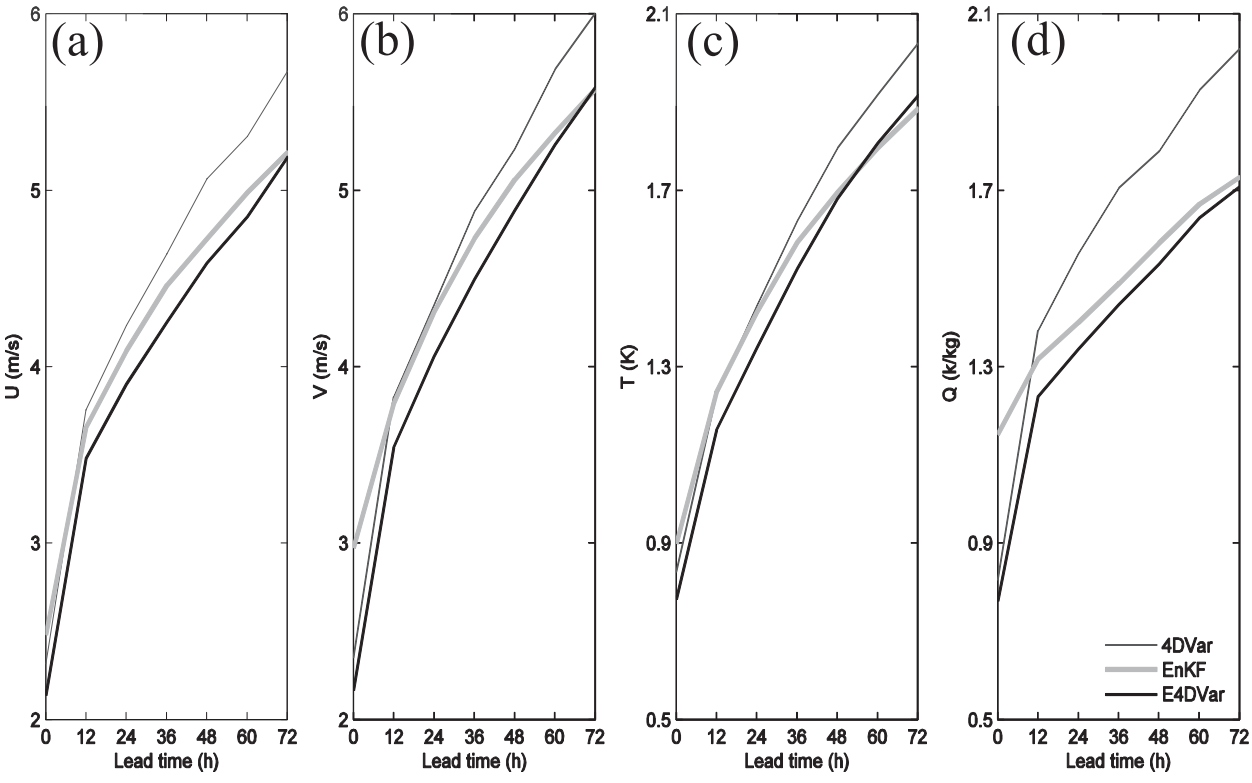

FIG. 9. Domain-averaged RMSEs further averaged over all 59 WRF forecasts of the month for each DA experiment at forecast lead times from 0 to 72 h evaluated every 12 h for (a) U (m s^{-1}), (b) V (m s^{-1}), (c) T (K), and (d) Q (g kg^{-1}).

in the DA process provides dramatic improvements over the variational methods, especially in the humidity field. Among all the DA methods, the E4DVar algorithm gives overall the best performance within a 72-h range (except for a slightly larger error in T than the EnKF after 60 h). For the hybrid system, more sources of flow-dependent information are used (i.e., the evolution of covariance is modeled by 4DVar within the assimilation window and the EnKF evolves the covariance from one window to the next; Lorenc 2003a). In addition, after the NMC- and ensemble-based background error covariance estimates are mixed, and propagated through tangent linear and adjoint models in the 4DVar, the impact of sampling errors is reduced (as shown in single-observation experiments), which makes the E4DVar more flexible for operational applications.

6. Sensitivity experiments

Given that E4DVar requires the coupling of EnKF and 4DVar methods, its performance is likely to depend on the configurations and quality of each of the two components. The number of empirical parameters used by both systems makes it impossible for us to exhaust all possible parameter configures, thus the control set of experiments presented in the previous sections may not be optimal (though they do represent our best effort). Nevertheless, in this section we will present the performance sensitivity to a couple of key configurations in the E4DVar system.

First, as mentioned in section 2 and discussed in Zhang et al. (2011), one of the key tunable parameters in the WRF-Var system is the variance magnitude of the background error covariance derived from the NMC method. A variance magnitude scale factor of 3.0 is used in both the control 4DVar and E4DVar experiments discussed above. The two left bars in Fig. 10 show that the control 4DVar performs marginally better than a configuration using the default value of 1.0 (much larger improvements are also seen for 3DVar with a variance factor of 3.0, not shown). The 12-h forecast of RM-DTE is used in Fig. 10. This sensitivity experiment suggests that the current E4DVAR may benefit from using a larger total variance magnitude in 4DVAR, but the overall improvement of the coupled system is likely due to its hybrid with the flow-dependent background error covariance derived from the EnKF.

We also examined the system's sensitivity to the coefficient β in (8), which selects the weights of the

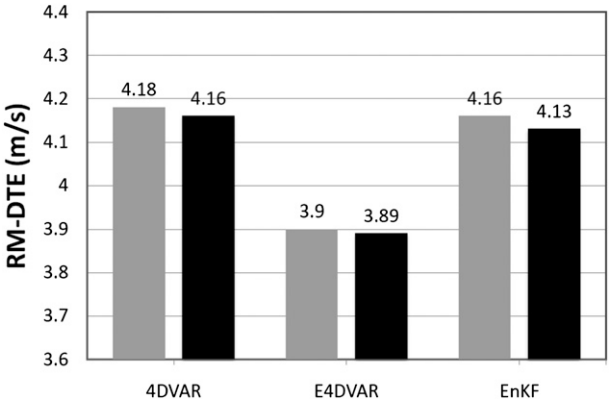

FIG. 10. The absolute 12-h forecast errors of different experiments in terms of RM-DTE (m s^{-1}). The black bars are the default experiments used in this study. The gray bars are the sensitivity experiments with different tunings: 1.0 variance scaling in 4DVar, 0.5 weighting parameter for E4DVar, and a single-physics scheme for EnKF in sequence.

NMC- and ensemble-based covariance in the E4DVar. A value of 0.8, which gives 80% of the weights to ensemble-based covariance, is used for the control E4DVar experiment though there is hardly much difference between using a value of 0.5 as shown in the two middle bars in Fig. 10.

The control EnKF and E4DVar experiments use a combination of physics parameterization schemes that differ between ensemble members as a means of treating model error. This multiphysics approach was found to have improved performance over identical configurations that used the same combination of physical parameterization in all ensemble members in Meng and Zhang (2008a,b). Likewise, a slightly better performance is observed for the control EnKF with a multiphysics ensemble over the cases that use a single-scheme ensemble (the two right bars in Fig. 10).

In summary, the coupled E4DVar system presented here is likely to be not quite sensitive to the few essential empirical configurations in the current application. If it can be generalized, that will be good news for its practicality in desiring more flexible operational systems.

7. Conclusions

This study explores the coupling of two state-of-the-art data assimilation algorithms in the context of regional WRF model configurations. To the best of our knowledge, this is the first successful implementation of a hybrid data assimilation approach that has two-way coupling of the EnKF and 4DVar methods in a limited-area weather prediction model, complementary to recent studies with a global model as in Buehner et al. (2010a,b). In this coupled DA system, denoted E4DVar, the EnKF and 4DVar run in parallel while intermittently exchanging information with each other. The multivariate, flow-dependent background error covariance estimated from the EnKF ensemble is used in the 4DVar minimization and the ensemble mean in the EnKF analysis is replaced by the 4DVar analysis, while the EnKF updates perturbations for the next cycle of ensemble forecasts. Therefore, the E4DVar can obtain flow-dependent information both from the explicit covariance matrix derived from ensemble forecasts as well as implicitly by the 4DVar trajectory.

The E4DVar is compared with the uncoupled 4DVar and EnKF over the contiguous United States for June 2003 to evaluate its performance in assimilating various conventional observations. Also presented is the importance of multivariate flow-dependent background error covariance exemplified by several single-observation experiments under different DA configurations. Single-observation experiments demonstrate that the E4DVar is capable of utilizing the time-evolving covariance through a combination of both explicit and implicit flow-dependent estimations.

By verifying the forecast from each analysis with standard sounding observations, it is found that the E4DVar substantially outperforms both the EnKF and 4DVar during this active summer month that featured several episodes of severe, convective weather. On average, the forecasts from the E4DVar analysis have considerably smaller errors than both of the stand-alone EnKF and 4DVar for up to 60-h lead forecast times. Moreover, it appears that the E4DVar may be less sensitive to DA configurations than both components of the system as the preliminary results shown in a set of single-observation experiments. The coupled system benefits from more flow-dependent information, a larger immunity to sampling error for a limited ensemble size, and enhanced capability in dealing with asynchronous and high-volume observations.

The computational cost of the E4DVar will be a concern for its full applications, where the major costs are from the iterative inner loops in the 4DVar and the sequential analysis in the EnKF. The 4DVar and EnKF have roughly 45- and 5-min wall-clock time for each analysis cycle, respectively, and such costs may increase dramatically for high-resolution modeling, especially in the 4DVar component. Several methods to minimize these costs include: (i) improve the efficiency of parallel computing of the related codes; (ii) use a coarse-resolution inner loop for 4DVar and EnKF analysis, so-called multi-incremental 4DVar (Courtier et al. 1994) and dual-resolution EnKF (Gao and Xue 2008); (iii) introduce a second outer loop in 4DVar with preconditioning from

the prestart, half-window analysis (refer to Fig. 1). These cost saving schemes will be tested in future experiments with higher resolution.

It is also worth noting that by no means can the current E4DVAR system claim to be the optimal configuration, partially due to the unaffordable high computational costs of exhaustive tuning and diagnostics. On the other hand, even if the E4DVAR system is likely not to be optimal as presented, we have demonstrated the E4DVAR can outperform both component systems of 4DVAR and EnKF, which have been well tuned, suggesting that there exists even greater space for the improvements for the coupled system in the future.

Acknowledgments. We thank Drs. Xiang-Yu Huang, Xin Zhang, and Chris Snyder at NCAR for their support with the algorithm development and their constructive comments. We also thank Jonathan Poterjoy for his proofreading of the manuscript. This work was supported by the Office of Naval Research Grants N000140910526 and the National Science Foundation Grant ATM-0840651.

REFERENCES

Andersson, E., M. Fisher, R. Munro, and R. A. McNally, 2000: Diagnosis of background error for radiances and other observable quantities in a variational data assimilation scheme, and the explanation of a case of poor convergence. ECMWF Tech. Memo. 296, Reading, United Kingdom, 22 pp.

Barker, D. M., W. Huang, Y.-R. Guo, A. J. Bourgeois, and Q. N. Xiao, 2004: A three-dimensional variational data assimilation system for MM5: Implementation and initial results. *Mon. Wea. Rev.,* **132,** 897–914.

Berre, L., 2000: Estimation of synoptic and mesoscale forecast error covariances in a limited area model. *Mon. Wea. Rev.,* **128,** 644–667.

Bishop, C. H., B. J. Etherton, and S. J. Majumdar, 2001: Adaptive sampling with the ensemble transform Kalman filter. Part I: Theoretical aspects. *Mon. Wea. Rev.,* **129,** 420–436.

Buehner, M., 2005: Ensemble-derived stationary and flow-dependent background-error covariances: Evaluation in a quasi-operational NWP setting. *Quart. J. Roy. Meteor. Soc.,* **131,** 1013–1043.

——, P. L. Houtekamer, C. Charette, H. L. Mitchell, and B. He, 2010a: Intercomparison of variational data assimilation and the ensemble Kalman filter for global deterministic NWP. Part I: Description and single-observation experiments. *Mon. Wea. Rev.,* **138,** 1550–1566.

——, ——, ——, ——, and ——, 2010b: Intercomparison of variational data assimilation and the ensemble Kalman filter for global deterministic NWP. Part II: One-month experiments with real observations. *Mon. Wea. Rev.,* **138,** 1567–1586.

Courtier, P., 1997: Dual formulation of four-dimensional variational data assimilation. *Quart. J. Roy. Meteor. Soc.,* **123,** 2449–2461.

——, J.-N. Thépaut, and A. Hollingsworth, 1994: A strategy for operational implementation of 4D-Var, using an incremental approach. *Quart. J. Roy. Meteor. Soc.,* **120,** 1367–1387.

Dowell, D. C., F. Zhang, L. J. Wicker, C. Snyder, and N. A. Crook, 2004: Wind and thermodynamic retrievals in the 17 May 1981 Arcadia, Oklahoma, supercell: Ensemble Kalman filter experiments. *Mon. Wea. Rev.,* **132,** 1982–2005.

Evensen, G., 1994: Sequential data assimilation with a nonlinear quasi-geostrophic model using Monte Carlo methods to forecast error statistics. *J. Geophys. Res.,* **99,** 10 143–10 162.

Fujita, T., D. J. Stensrud, and D. C. Dowell, 2007: Surface data assimilation using an ensemble Kalman filter approach with initial condition and model physics uncertainties. *Mon. Wea. Rev.,* **135,** 1846–1868.

Gao, J., and M. Xue, 2008: An efficient dual-resolution approach for ensemble data assimilation and tests with assimilated Doppler radar data. *Mon. Wea. Rev.,* **136,** 945–963.

Gaspari, G., and S. E. Cohn, 1999: Construction of correlation functions in two and three dimensions. *Quart. J. Roy. Meteor. Soc.,* **125,** 723–757.

Gauthier, P., and J. N. Thépaut, 2001: Impact of the digital filter as a weak constraint in the preoperational 4D-Var assimilation system of Météo-France. *Mon. Wea. Rev.,* **129,** 2089–2102.

——, M. Tanguay, S. Laroche, and S. Pellerin, 2007: Extension of 3DVAR to 4DVAR: Implementation of 4DVAR at the Meteorological Service of Canada. *Mon. Wea. Rev.,* **135,** 2339–2364.

Grell, G. A., and D. Dévényi, 2002: A generalized approach to parameterizing convection combining ensemble and data assimilation techniques. *Geophys. Res. Lett.,* **29,** 1693, doi:10.1029/2002GL015311.

Guo, Y.-R., Y.-H. Kuo, J. Dudhia, D. Parsons, and C. Rocken, 2000: Four-dimensional variational data assimilation of heterogeneous mesoscale observations for a strong convective case. *Mon. Wea. Rev.,* **128,** 619–643.

Hamill, T. M., and C. Snyder, 2000: A hybrid ensemble Kalman filter 3D variational analysis scheme. *Mon. Wea. Rev.,* **128,** 2905–2919.

Hayden, C. M., and R. J. Purser, 1995: Recursive filter objective analysis of meteorological fields: Applications to NESDIS operational processing. *J. Appl. Meteor.,* **34,** 3–15.

Honda, Y., M. Nishijima, K. Koizumi, Y. Ohta, K. Tamiya, T. Kawabata, and T. Tsuyuki, 2005: A pre-operational variational data assimilation system for a non-hydrostatic model at the Japan Meteorological Agency: Formulation and preliminary results. *Quart. J. Roy. Meteor. Soc.,* **131,** 3465–3475.

Hong, S.-Y., J. Dudhia, and S.-H. Chen, 2004: A revised approach to ice microphysical processes or the bulk parameterization of clouds and precipitation. *Mon. Wea. Rev.,* **132,** 103–120.

Houtekamer, P. L., H. L. Mitchell, and X. Deng, 2009: Model error representation in an operational ensemble Kalman filter. *Mon. Wea. Rev.,* **137,** 2126–2143.

Huang, X.-Y., X. Yang, N. Gustafsson, K. Mogensen, and M. Lindskog, 2002: Four-dimensional variational data assimilation for a limited area model. HIRLAM Tech. Rep. 57, 41 pp.

Huang, X. Y., and Coauthors, 2009: Four-dimensional variational data assimilation for WRF: Formulation and preliminary results. *Mon. Wea. Rev.,* **137,** 299–314.

Liu, C., Q. Xiao, and B. Wang, 2008: An ensemble-based four-dimensional variational data assimilation scheme. Part I: Technical formulation and preliminary test. *Mon. Wea. Rev.,* **136,** 3363–3373.

——, ——, and ——, 2009: An ensemble-based four-dimensional variational data assimilation scheme. Part II: Observing System Simulation Experiments with Advanced Research WRF (ARW). *Mon. Wea. Rev.,* **137,** 1687–1704.

Lorenc, A. C., 2003a: The potential of the ensemble Kalman filter for NWP—A comparison with 4D-VAR. *Quart. J. Roy. Meteor. Soc.,* **129,** 3183–3203.

——, 2003b: Modelling of error covariances by 4D-Var data assimilation. *Quart. J. Roy. Meteor. Soc.,* **129,** 3167–3182.

——, and Coauthors, 2000: The Met. Office global three-dimensional variational data assimilation scheme. *Quart. J. Roy. Meteor. Soc.,* **126,** 2991–3012.

Meng, Z., and F. Zhang, 2007: Test of an ensemble Kalman filter for mesoscale and regional-scale data assimilation. Part II: Imperfect-model experiments. *Mon. Wea. Rev.,* **135,** 1403–1423.

——, and ——, 2008a: Test of an ensemble Kalman filter for mesoscale and regional-scale data assimilation. Part III: Comparison with 3DVAR in a real-data case study. *Mon. Wea. Rev.,* **136,** 522–540.

——, and ——, 2008b: Test of an ensemble Kalman filter for mesoscale and regional-scale data assimilation. Part IV: Performance over a warm-season month of June 2003. *Mon. Wea. Rev.,* **136,** 3671–3682.

Miyoshi, T., Y. Sato, and T. Kadowaki, 2010: Ensemble Kalman filter and 4D-Var intercomparison with the Japanese Operational Global Analysis and Prediction System. *Mon. Wea. Rev.,* **138,** 2846–2866.

Navon, I. M., D. N. Daescu, and Z. Liu, 2005: The impact of background error on incomplete observations for 4D-Var data assimilation with the FSU GSM. *Lect. Notes Comput. Sci.,* **3515,** 837–844.

Noh, Y., W. G. Cheon, S. Y. Hong, and S. Raasch, 2003: Improvement of the K-profile model for the planetary boundary layer based on large eddy simulation data. *Bound.-Layer Meteor.,* **107,** 421–427.

Parrish, D. F., and J. C. Derber, 1992: The National Meteorological Center's spectral statistical-interpolation analysis system. *Mon. Wea. Rev.,* **120,** 1747–1763.

Rabier, F., J.-N. Thépaut, and P. Courtier, 1998: Extended assimilation and forecast experiments with a four-dimensional variational assimilation system. *Quart. J. Roy. Meteor. Soc.,* **124,** 1861–1887.

——, H. Järvinen, E. Klinker, J.-F. Mahfouf, and A. Simmons, 2000: The ECMWF operational implementation of four dimensional variational assimilation. *Quart. J. Roy. Meteor. Soc.,* **126,** 1143–1170.

Skamarock, W. C., J. B. Klemp, J. Dudhia, D. O. Gill, D. M. Barker, W. Wang, and J. G. Powers, 2005: A description of the advanced research WRF version 2. NCAR Tech. Note TN-468+STR, 88 pp.

Snyder, C., and F. Zhang, 2003: Tests of an ensemble Kalman filter for convective-scale data assimilation. *Mon. Wea. Rev.,* **131,** 1663–1677.

Sun, J., and N. A. Crook, 1997: Dynamical and microphysical retrieval from Doppler radar observations using a cloud model and its adjoint. Part I: Model development and simulated data experiments. *J. Atmos. Sci.,* **54,** 1642–1661.

Thépaut, J.-N., P. Courtier, G. Belaud, and G. Lemaitre, 1996: Dynamic structure functions in a four-dimensional variational assimilation: A case study. *Quart. J. Roy. Meteor. Soc.,* **122,** 535–561.

Tong, M., and M. Xue, 2005: Ensemble Kalman filter assimilation of Doppler radar data with a compressible nonhydrostatic model: OSS experiments. *Mon. Wea. Rev.,* **133,** 1789–1807.

Torn, R. D., G. J. Hakim, and C. Snyder, 2006: Boundary conditions for a limited-area ensemble Kalman filter. *Mon. Wea. Rev.,* **134,** 2490–2502.

Wang, X., C. Snyder, and T. M. Hamill, 2007: On the theoretical equivalence of differently proposed ensemble–3DVAR hybrid analysis schemes. *Mon. Wea. Rev.,* **135,** 222–227.

——, D. M. Barker, C. Snyder, and T. M. Hamill, 2008a: A hybrid ETKF–3DVAR data assimilation scheme for the WRF model. Part I: Observation System Simulation Experiment. *Mon. Wea. Rev.,* **136,** 5116–5131.

——, ——, ——, and ——, 2008b: A hybrid ETKF–3DVAR data assimilation scheme for the WRF model. Part II: Real observation experiments. *Mon. Wea. Rev.,* **136,** 5132–5147.

——, T. M. Hamill, J. S. Whitaker, and C. H. Bishop, 2009: A comparison of the hybrid and EnSRF analysis schemes in the presence of model error due to unresolved scales. *Mon. Wea. Rev.,* **137,** 3219–3232.

Whitaker, J. S., T. M. Hamill, X. Wei, Y. Song, and Z. Toth, 2008: Ensemble data assimilation with the NCEP global forecast system. *Mon. Wea. Rev.,* **136,** 463–482.

Xu, L., T. Rosmond, and R. Daley, 2005: Development of NAVDAS-AR: Formulation and initial tests of the linear problem. *Tellus,* **57A,** 546–559.

Zhang, F., C. Snyder, and R. Rotunno, 2002: Mesoscale predictability of the ''surprise'' snowstorm of 24–25 January 2000. *Mon. Wea. Rev.,* **130,** 1617–1632.

——, ——, and J. Sun, 2004: Impacts of initial estimate and observation availability on convective-scale data assimilation with an ensemble Kalman filter. *Mon. Wea. Rev.,* **132,** 1238–1253.

——, Z. Meng, and A. Aksoy, 2006: Test of an ensemble Kalman filter for mesoscale and regional-scale data assimilation. Part I: Perfect-model experiments. *Mon. Wea. Rev.,* **134,** 722–736.

——, M. Zhang, and J. A. Hansen, 2009: Coupling ensemble Kalman filter with four- dimensional variational data assimilation. *Adv. Atmos. Sci.,* **26,** 1–8.

Zhang, M., F. Zhang, X. Y. Huang, and X. Zhang, 2011: Intercomparison of an ensemble Kalman filter with three- and four-dimensional variational data assimilation methods in a limited-area model over the month of June 2003. *Mon. Wea. Rev.,* **139,** 566–572.

Zou, X., 1997: Tangent linear and adjoint of ''on/off'' processes and their feasibility for use in 4-dimensional variational data assimilation. *Tellus,* **49A,** 3–31.

——, and Y.-H. Kuo, 1996: Rainfall assimilation through an optimal control of initial and boundary conditions in a limited-area mesoscale model. *Mon. Wea. Rev.,* **124,** 2859–2882.

Zupanski, D., D. F. Parrish, E. Rogers, and G. DiMego, 2002: Four-dimensional variational data assimilation for the blizzard of 2000. *Mon. Wea. Rev.,* **130,** 1967–1988.

Zupanski, M., D. Zupanski, T. Vukicevic, K. Eis, and T. V. Haar, 2005: CIRA/CSU four-dimensional variational data assimilation system. *Mon. Wea. Rev.,* **133,** 829–843.